PHYSICAL REVIEW C VOLUME 25, NUMBER 6 JUNE 1982

Coulomb final state interaction and the charge effect in heavy ion projectile fragmentation at intermediate energies

Cheuk-Yin Wong
Physics Division, Oak Ridge National Laboratory, Oak Ridge, Tennessee 37830

K. Van Bibber
Department of Physics, Stanford University, Stanford, California 94305
(Received 30 September 1981)

In intermediate energy heavy-ion projectile fragmentation the width of the transverse momentum distribution for a given fragment mass depends on the charge number of the fragment. The greater the charge number, the smaller is the width of the transverse momentum distribution. Such a charge effect may be explained in terms of a Coulomb final state interaction between the fragment and the protons dissociated from the projectile. With simple assumptions concerning the fragmentation process, analytic expressions for the momentum dispersions are obtained and are found to give good agreement with experimental results.

[NUCLEAR REACTIONS Heavy ions. Projectile fragmentation. Intermediate energy. Coulomb final state interaction. Calculate $\sigma_\perp^2$, $\sigma_\parallel^2$.]

Ideally, fragment momentum distributions in projectile fragmentation provide useful information on the nuclear ground state. The dispersions of the fragment momentum distributions measure the magnitude of the Fermi momentum.[1,2] The high energy end of the fragment spectra may reflect the high momentum tail of subsystems inside a nucleus.[3–5] The momentum distribution for single nucleon removal exhibits sensitivity to the Wigner function on the nuclear surface.[6]

In reality, the connection between measured momentum spectra and nuclear ground state properties is modified by important corrections. The Pauli exclusion principle has the effect of reducing the width of the momentum distribution.[7] The angular distributions of nuclear fragments at intermediate energies are influenced by the deflection of the projectile in the field of the target.[8] Final state interactions are expected to play a role in the observed fragment momentum distributions.

In this regard, Legrain[9] has recently pointed out striking systematics in fragment angular distributions for $E/A \simeq 100$ MeV/nucleon which seems to be a general feature for all existing data: ^{40}Ar + C at 118 MeV/nucleon[8,10]; ^{16}O + Al, Au at 90, 100, and 120 MeV/nucleon[8,11]; and ^{12}C + Ag at 86 MeV/nucleon.[12] In the projectile fragmentation region for these reactions, the widths of the angular distributions for fragments with different masses follow approximately the description of an intrinsic momentum distribution modified by orbital dispersion.[8] However, for fragments with the same mass but different charge numbers Z_F, there is a small but systematic decrease in the widths as the charge number increases. For the longitudinal momentum distributions, there is some hint that a similar charge effect is present but with a much reduced magnitude.[13,14]

Figure 1 shows data for ^{40}Ar and ^{16}O projectiles in terms of the dispersion of the transverse momentum distribution $\sigma_\perp$. The regular progression of widths through the valley of stability for all isobars rules out any explanations based on Q values. Differing Fermi momenta for neutrons and protons must also be excluded, as the required difference ($\Delta\sigma_0 \simeq 25$ MeV/c) is far too large to be reconciled with other existing data. In any case, such a difference would produce a corresponding dependence in the longitudinal distributions as well. This, however, is not observed. Because of the charge dependence of the effect, a Coulomb final state interaction is strongly suggested.

It is evident that the Coulomb interaction between the projectile spectator and the target cannot explain the effect, as the transverse widths for ^{16}O + Al are essentially identical to those with the Au target, whereas the charges of the targets differ greatly. What remains is the possibility of a

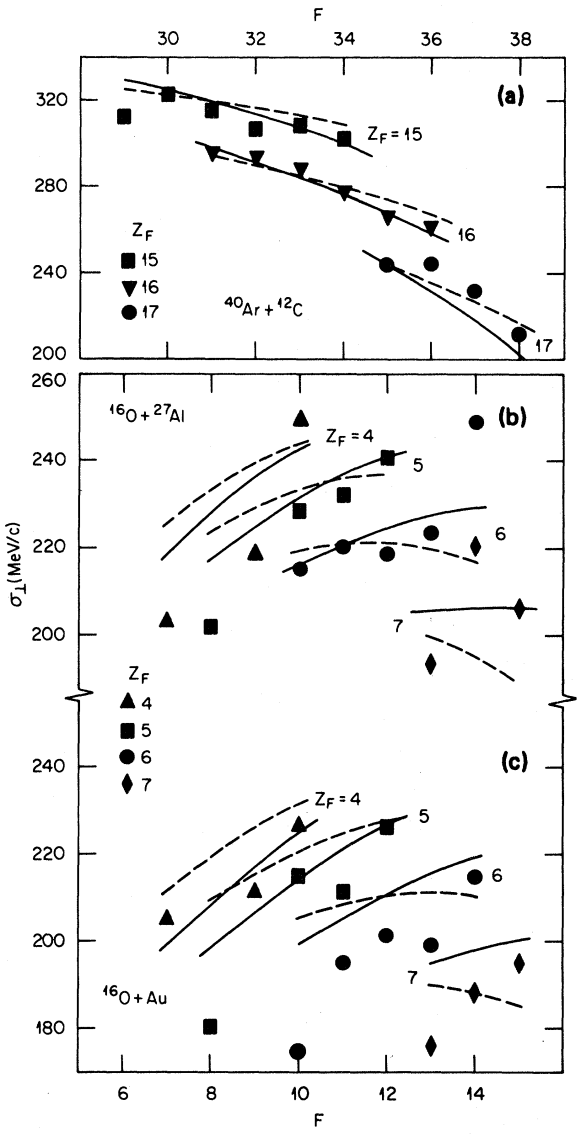

FIG. 1. Transverse momentum widths $\sigma_\perp$ as a function of Z_F and F for the reactions (a) ^{40}Ar + C, 118 MeV/nucleon (Ref. 10); (b) ^{16}O + Al, 100 MeV/nucleon (Ref. 11); (c) ^{16}O + Au 100 MeV/nucleon (Ref. 11). The lines represent the calculated transverse momenta with the Coulomb final state interaction as described in the text.

Coulomb final state interaction between the projectile spectator (the observed fragment) and the nuclear matter removed from it.

In order to give a quantitative estimate of the effect of the Coulomb final state interaction, it is necessary to construct a concrete picture of the process. Two scenarios may be shown to be incompatible with data, at least as the predominant mechanism, leaving a third plausible description. If the projectile were to equilibrate after scattering and then only later decay into the observed fragment, the effect due to the final state interaction will be independent of direction. This is not the case, judging from the weak charge effect in the longitudinal direction contrasted with the strong charge effect in the transverse direction. Also, if the projectile of charge number Z_A were to break up into two massive fragments, the final-state interaction would contribute to the width as $Z_F(Z_A - Z_F)$. This is also not the case, as the width always decreases with increasing Z_F.

Physically, one expects a fragmentation process to be a prompt peripheral process, with the observed fragment being the spectator part of the parent projectile nucleus. The participant part of the parent nucleus lies in the region where the nuclear matter of the projectile and target overlap. After such a peripheral encounter, the participant part of the projectile is likely to dissociate into a gas which moves with only a small momentum relative to the observed fragment (Fig. 2). Experimental evidence for such a behavior comes from the in-plane 180° correlation which exists in the laboratory system between the slow target fragments and the fast charged particles which are presumably the target participants in a peripheral collision.[15] This correlation data, on which our model is based, cannot be explained by the conventional fireball model.[15] Rather, it is plausible for peripheral collisions in which the participant nucleons traverse only a short distance through the other nucleus that they could not be brought to rest to form a fireball. Theoretical calculations with nuclear hydrodynamics, which can only be used as a very rough qualitative guide, also exhibit the nucleonic gas clouds following the spectator pieces for sufficiently peripheral collisions.[16,17]

In our model, the Coulomb final-state interaction consists of the vector sum of all Coulomb kicks exerted between each dissociated proton in the gas and the fragment. Nevertheless, the proton gas will not be distributed isotropically with respect to the fragment, but rather will be localized on the same side as the target nucleus. For simplicity, we assume that the dissociated nucleons lie in the half-space opposite the projectile spectator, and the plane dividing participants and spectator is normal to the transverse momentum the projectile receives in the field of the target nucleus, $\vec{D}_\perp$.

The fragment momentum $\vec{P}_F$ (referred to the pro-

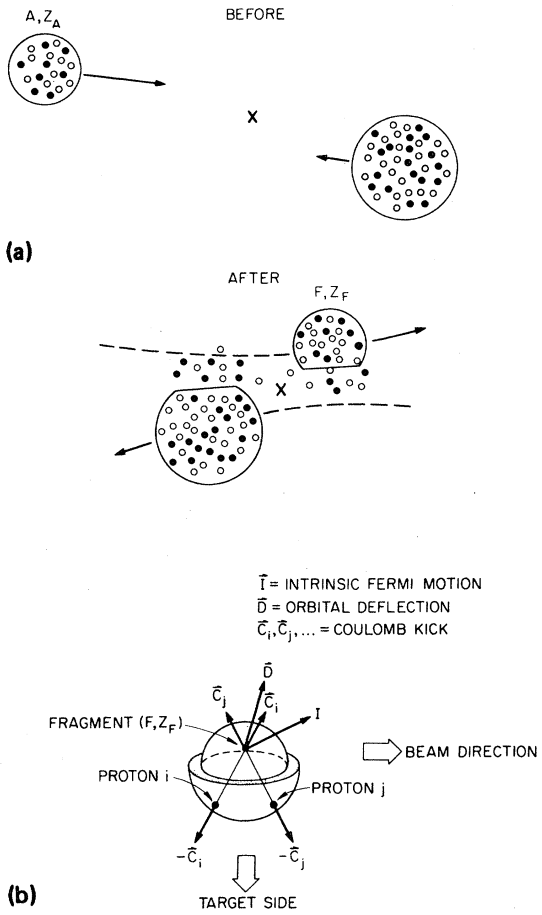

FIG. 2. (a) Schematic representation of the fragmentation process in the center of mass system. (b) Momentum diagram indicating the contributions due to intrinsic Fermi motion $\vec{I}$, orbital deflection $\vec{D}$, and Coulomb final state interaction $\vec{C}_i$ in the projectile center-of-mass system.

jectile center-of-mass system) arises from three types of contributions in the present treatment. The distribution of the intrinsic momentum $\vec{I}$ due to the Fermi motion of nucleons prior to collision is taken to be

$$P_I(\vec{I})=\frac{1}{(\sqrt{2\pi}\sigma_I)^3}\exp(-I^2/2\sigma_I^2)\ , \tag{1}$$

where[1]

$$\sigma_I^2=F(A-F)\sigma_0^2/(A-1)\ , \tag{2}$$

with A the projectile mass number, and σ_0 related to the Fermi momentum p_f by $\sigma_0^2=p_f^2/5$. The orbital motion due to any dynamical deflection of the projectile in the field of the target contributes a momentum $\vec{D}$ with a distribution

$$P_D(\vec{D})=\frac{1}{(\sqrt{2\pi})^3\sigma_{D\perp}^2\sigma_{DZ}} \times\exp[-\vec{D}_\perp^2/2\sigma_{D\perp}^2-D_Z^2/2\sigma_{DZ}^2]\ , \tag{3}$$

where $\sigma_{D\perp}$ is shown to be[8]

$$\sigma_{D\perp}^2=\frac{F(F-1)}{A(A-1)}\sigma_{1\perp}^2 \tag{4}$$

and similarly, we can show that σ_{DZ} for a fragment with mass F is given by

$$\sigma_{DZ}^2=\frac{F(F-1)}{A(A-1)}\sigma_{1Z}^2\ . \tag{5}$$

Here, $\sigma_{1\perp}$ and σ_{1Z} measure the degree of the dispersion, respectively, in the transverse and the longitudinal directions due to the orbital deflection of the projectile in the field of the target nucleus. Finally, the Coulomb final-state interaction between ith dissociated proton and the fragment contributes a momentum $\vec{C}_i$ with $i=1,\ldots,Z_A-Z_F$. Based on the description of the fragmentation process discussed above, the distribution of $\vec{C}_i$ is

$$P_C(\vec{C}_i)=\frac{1}{2\pi}\theta(\pm\vec{C}_i\cdot\vec{D}_\perp)\delta(|\vec{C}_i|-C_0)\ . \tag{6}$$

Here, the step function specifies that the Coulomb kick is distributed on a half-sphere either on the same side or the opposite side of the transverse component of the orbital deflection vector $\vec{D}_\perp$, depending on the sign of the scattering angle. The sign inside the step function is positive for positive angle scattering and negative for negative angle scattering. We can estimate the magnitude C_0 by energy considerations as follows:

$$\frac{C_0^2}{2m}+\frac{C_0^2}{2m_F}=\frac{Z_F\cdot1\cdot e^2}{R}\ , \tag{7}$$

where m and m_F are the mass of a proton and the fragment, respectively, and R, parametrized as $R=r_0A^{1/3}$, is the mean initial separation between a dissociated proton and the fragment. We therefore obtain

$$C_0=\sqrt{2mZ_Fe^2F/(F+1)R}\ . \tag{8}$$

The momentum distribution for the fragment is therefore

$$W(\vec{P}_F)=\prod_{i=1}^{Z_A-Z_F}\int d\vec{I}\,d\vec{D}\,d\vec{C}_iP_I(\vec{I})P_D(\vec{D})P_C(\vec{C}_i)\delta\left[\vec{P}_F-\vec{I}-\vec{D}-\sum_{j=1}^{Z_A-Z_F}\vec{C}_j\right] \tag{9}$$

from which are derived the longitudinal and transverse dispersions,

$$\sigma_{||}^2(F,Z_F)=\sigma_I^2+\sigma_{DZ}^2+\tfrac{1}{3}(Z_A-Z_F)C_0^2\,, \tag{10}$$

$$\sigma_{\perp}^2(F,Z_F)=\sigma_I^2+\sigma_{D\perp}^2\pm\frac{\sqrt{2\pi}}{4}(Z_A-Z_F)C_0\sigma_{D\perp} +C_0^2(Z_A-Z_F)\left[\frac{1}{3}+\frac{(Z_A-Z_F-1)}{8}\right], \tag{11}$$

where the positive (negative) sign indicates positive (negative) angle scattering. We see that the Coulomb final-state interaction increases $\sigma_{||}^2$ by a term proportional to (Z_A-Z_F) (random walk with zero mean), but increases $\sigma_{\perp}^2$ by a term proportional approximately to $(Z_A-Z_F)^2$ (random walk with nonzero mean). The charge effect is larger in the transverse direction than in the longitudinal direction, when the scattering angle is positive.

We analyze the experimental data of ^{16}O at 100 MeV/A, and ^{40}Ar at 118 MeV/A in terms of Eqs. (10) and (11) and assume positive angle scattering. The $\sigma_{\perp}$ data for ^{40}Ar are very satisfactorily reproduced with $\sigma_0=80$ MeV/c, $\sigma_{1\perp}=150$ MeV/c, and a radius parameter $r_0=1.0$ fm [solid curves in Fig. 1(a)]; alternatively, comparable agreement is achieved with $\sigma_0=90$ MeV/c, $\sigma_{1\perp}=150$ MeV/c, and $r_0=1.2$ fm [dashed curves in Fig. 1(a)]. Only qualitative agreement for ^{16}O is attained; the solid (dashed) curves in Fig. 1 represent the calculations for $\sigma_0=80$ (70), $\sigma_{1\perp}=150$ (170), $r_0=1.0$ (1.0) for the Al target, and 70 (60), 150 (175), 1.0 (1.2) for the Au target. The assumption of a negative angle scattering leads to a very small charge effect and is inconsistent with the data.

The longitudinal momentum distributions are affected also by the presence of the Coulomb final-state interaction. Again, the greater the charge number, the larger is the width of the longitudinal momentum distribution. This charge effect is, however, very small, as one observes in Fig. 3 where we show the dispersion $\sigma_{||}$ for ^{40}Ar + ^{12}C and ^{16}O + Al calculated with the set of parameters $\sigma_0=80$ MeV/c and $r_0=1.0$ fm inferred from the transverse momentum distributions, and $\sigma_{1Z}=0$.[18] There is qualitative agreement with data, and no charge effect exceeding experimental errors is predicted.[19] Thus, the inclusion of the Coulomb final-state interaction is consistent with both the transverse and the longitudinal momentum data.

As is evident from Eq. (10), the presence of the Coulomb final-state interaction gives an overall

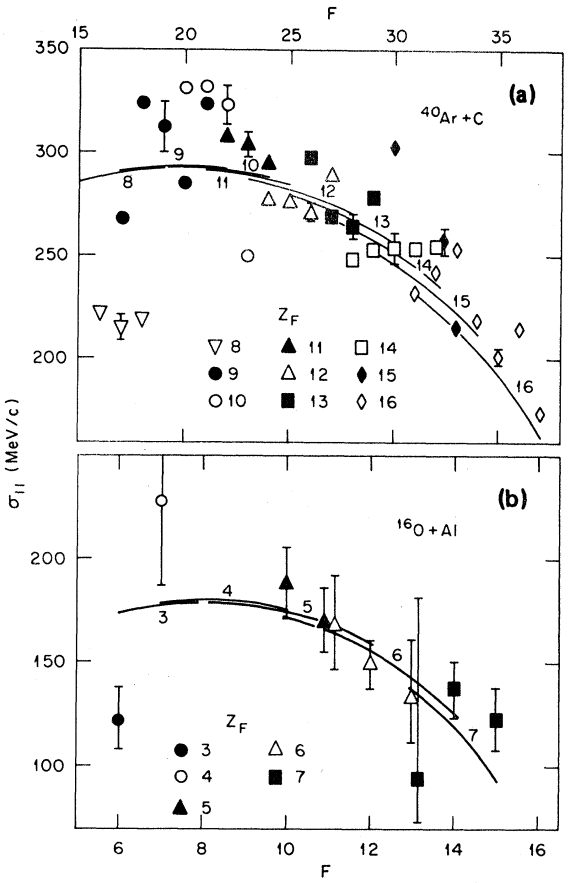

FIG. 3. Experimental and calculated longitudinal momentum widths $\sigma_{||}$ as a function of Z_F and F for (a) ^{40}Ar + C, 213 MeV/nucleon (Ref. 13); and (b) ^{16}O + Al, 92.5 MeV/nucleon (Ref. 8). The lines indicate the calculated $\sigma_{||}$ with $\sigma_0=80$ MeV/c and $r_0=1.0$ fm for both systems.

broadening of the longitudinal momentum distributions. As far as the overall broadening is concerned, the case of ^{40}Ar + ^{12}C for $\sigma_0=80$ MeV/c with the Coulomb final-state interaction represented by $r_0=1.0$ fm can be approximated as a case without the Coulomb final-state interaction but with an effective intrinsic momentum dispersion $\sigma_0'=92$ MeV/c, essentially the result of 94 ± 5 MeV/c determined experimentally in Ref. 13. Similarly, the overall increase of $\sigma_{||}$ for ^{16}O + C due to the Coulomb final-state interaction with $\sigma_0=80$ MeV/c and $r_0=1.0$ fm can be approximated as a case without the Coulomb final-state interaction but with an effective intrinsic momentum dispersion $\sigma_0'=86$ MeV/c, in agreement with the dispersion determined in Refs. 8 and 14. The small value of the intrinsic momentum dispersion σ_0 may

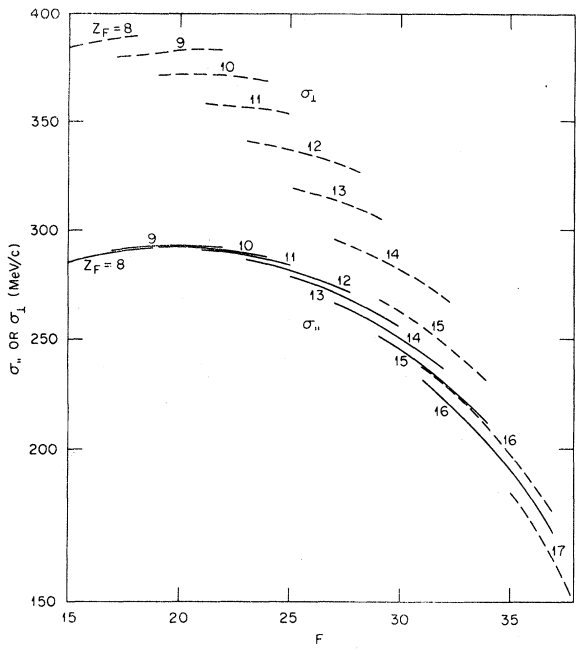

FIG. 4. Predictions on $\sigma_{\perp}$ and $\sigma_{||}$ for the fragmentation of ^{40}Ar in the high energy limit when $\sigma_{1\perp}=\sigma_{1Z}=0$. They are calculated with $\sigma_0=80$ MeV/c and $r_0=1.0$ fm.

be due to Pauli suppression, as explained previously.[7]

The overall enhancement of the transverse momentum distributions due to orbital dispersion has been previously pointed out, and the magnitude of the effect estimated in a simple picture.[8] There, the refraction of the projectile in the Coulomb-nuclear field of the target was calculated for a purely real attractive potential, implying largely negative angle scattering. It is to be noted, however, that the contribution to the transverse width associated with *any* projectile-target interaction is a positive-definite quantity; and, in fact, the charge effect strongly suggests that the scattering is predominantly to positive angles.

It is interesting to note that the effect of the Coulomb repulsion on the transverse widths manifests itself in Eq. (11) not only in a term proportional to $(Z_A-Z_F)^2$, but also in a cross term with the transverse orbital dispersion. This latter term, in fact, dominates at these lower energies for ejectiles not far removed from the projectile mass where the orbital dispersion is known to be significant. Nevertheless, even in the limit of no such dispersion, substantial differences are expected between $\sigma_{\perp}$ and $\sigma_{||}$. Figure 4 shows the predictions for ^{40}Ar with $\sigma_D=80$ MeV/c, $\sigma_{1\perp}=\sigma_{1Z}=0$. This limit is probably realized for the fragmentation of ^{40}Ar at high energies.

In summary, the charge dependence seen in fragment angular distributions at intermediate energies is plausibly shown to result from a Coulomb final-state interaction with the protons dissociated from the projectile. Although the present data in no way unambiguously determine the details of the spatial and momentum distributions of the system after interaction, the mere observation of the charge behavior already indicates that nucleon removal is predominantly prompt in fragmentation. Furthermore, it appears necessary that the fragments are ejected to the same side of the projectile in its interaction with the target, while the dissociated nucleons are ejected on the side of the target, as expected, on simple geometrical grounds.

We acknowledge useful discussions with R. Legrain, H. Nifenecker, T. J. M. Symons, D. K. Scott, G. Bertsch, and H. Gutbrod. This research was supported in part by the Division of Basic Energy Sciences, U. S. Department of Energy, under Contract W-7405-eng-26 with the Union Carbide Corporation.

[1]A. S. Goldhaber, Phys. Lett. 53B, 306 (1974).
[2]H. Feshbach and K. Huang, Phys. Lett. 47B, (1973).
[3]L. M. Anderson, Ph.D. thesis, University of California, Berkeley, 1977, Report No. LBL-6769.
[4]C. Y. Wong and R. Blankenbecler, Phys. Rev. C 22, 2433 (1980).
[5]J. V. Geaga, S. A. Chessin, J. Y. Grossiord, J. W. Harris, D. L. Hendrie, L. S. Schroeder, R. N. Treuhaft, and K. Van Bibber, Phys. Rev. Lett. 45, 1993 (1980).
[6]J. Hüfner and M. C. Nemes, Phys. Rev. C 23, 2538 (1981).
[7]G. Bertsch, Phys. Rev. Lett. 46, 472 (1981).
[8]K. Van Bibber, D. L. Hendrie, D. K. Scott, H. H. Wieman, L. S. Schroeder, J. V. Geaga, S. A. Chessin, R. Treuhaft, J. Y. Grossiord, J. O. Rasmussen, and C. Y. Wong, Phys. Rev. Lett. 43, 840 (1979).
[9]R. Legrain, private communication.
[10]R. Legrain, T. C. Awes, H. J. Crawford, C. K. Gelbke, D. E. Greiner, H. H. Heckman, J. M. Kidd, P. J. Lindstrom, J. Mahoney, D. K. Scott, T. J. M. Symons, and G. D. Westfall, Proceedings of the International Conference on Nuclear Physics, Berkeley, 1980, Report No. LBL-11118, p. 532.

[11]J. Silk *et al.* (unpublished).
[12]N. Nifenecker, private communication.
[13]Y. P. Viyogi, T. J. M. Symons, P. Doll, D. E. Greiner, H. H. Heckman, D. L. Hendrie, P. J. Lindstrom, J. Mahoney, D. K. Scott, K. Van Bibber, G. D. Westfall, H. Wieman, H. J. Crawford, C. McParland, and C. K. Gelbke, Phys. Rev. Lett. 42, 33 (1979).
[14]D. E. Greiner, P. J. Lindstrom, H. H. Heckman, Bruce Cork, and F. S. Bieser, Phys. Rev. Lett. 35, 152 (1975).
[15]W. G. Meyer, H. H. Gutbrod, Ch. Lukner, and A. Sandoval, Phys. Rev. C 22, 179 (1980).
[16]H. H. K. Tang, Ph.D. thesis, Yale University, 1979 (unpublished).
[17]A. A. Amsden, F. H. Harlow, and J. R. Nix, Phys. Rev. C 15, 2059 (1977); J. Kapusta and D. Strottman, Phys. Lett. 106B, 33 (1981).
[18]In fitting the data of Fig. 3, it is not necessary to introduce an orbital dispersion in the longitudinal direction for ^{40}Ar + C and ^{16}O + Al. However, there is some experimental evidence for the presence of longitudinal orbital dispersion of the form Eq. (5) in the collision of ^{12}C + ^{12}C [J. Mougey *et al.*, Phys. Lett. 105B, 25 (1981)]. The presence of such a term is, however, given an alternative explanation as arising from inelastic scattering.
[19]The data for ^{40}Ar + C, 213 MeV/nucleon (Ref. 13) are shown rather than that at 118 MeV/nucleon (Ref. 10), as they encompass a much broader range of fragmentation products and with considerably smaller error assignments. Although the $\sigma_{||}(F,Z_F)$ of Ref. 10 are systematically larger than those of Ref. 13, no dependence on the fragment charge is seen in these data either.